



Partial oxidation of methane over $\text{Ni}^0/\text{La}_2\text{O}_3$ bifunctional catalyst IV: Simulation of methane total oxidation, dry reforming and partial oxidation using the Quasi-Steady State Approximation



Tri Huu Nguyen ^{a,c,d,*}, Agata Łamacz ^{b,**}, Andrzej Krztoń ^{c,1}, Gérald Djéga-Mariadassou ^{e,2}

^a Saigon University, Faculty of Pedagogy of Natural Sciences, 273 An Duong Vuong Dist.5, HCMC, Vietnam

^b Wroclaw University of Technology, Division of Chemistry and Technology of Fuels, Gdanska 7/9, 50-344 Wroclaw, Poland

^c Centre of Polymer and Carbon Materials Polish Academy of Sciences, M. Curie-Skłodowskiej 34, 41-819 Zabrze, Poland

^d Silesian University of Technology, Faculty of Chemistry, M. Strzody 9, 44-100 Gliwice, Poland

^e University Pierre et Marie Curie, Paris, France

ARTICLE INFO

Article history:

Received 4 April 2016

Received in revised form 6 June 2016

Accepted 10 June 2016

Available online 23 June 2016

Keywords:

Kinetic simulation

Quasi-Steady State Approximation

Methane total oxidation

Methane dry reforming

Rate determining cycle of POM

ABSTRACT

Simulations of methane total oxidation (TOM) at 873 K on La_2O_3 and dry reforming (DRM) at 693 K reactions over $\text{Ni}^0/\text{La}_2\text{O}_3$ were calculated for low and high conversions of reactants, based on experimental power rate law equations described in a previous paper and classical kinetics. According to Boudart's school approach of Classical Kinetics, kinetic rate equations of TOM and DRM reactions were then established based on the Quasi-Steady State Approximation (QSSA) theory. The concept of two-step sequences was used for TOM and DRM which occur in the indirect process of partial oxidation of methane (POM). The QSSA simulation of POM process was subsequently developed at 1053 K and compared to the simulation of TOM, at the same temperature, to kinetically demonstrate that the TOM catalytic cycle is the rate determining cycle (rdc) of the POM process. Synthesis of a novel POM catalyst in the future can be based on the present model and conclusion, taking into account that the methane combustion reaction provides the rate determining catalytic cycle (rdc) of the overall POM process.

© 2016 Elsevier B.V. All rights reserved.

1. Introduction and background

In a 1st previous paper [1] the indirect model has been considered for the POM process based on 3 catalytic cycles turning over $\text{Ni}^0/\text{La}_2\text{O}_3$ a bifunctional catalyst. The corresponding 3 overall reactions are:

- Total oxidation of methane (TOM) over an oxide (here La_2O_3);
- Dry Reforming of methane (DRM) over Ni^0 , CO_2 being delivered by TOM;
- Steam Reforming of methane (SRM) over Ni^0 , H_2O being delivered by TOM.

Both DRM and SRM are kinetically coupled due to the same common elementary steps of methane activation by successive dehydrogenation steps over Ni^0 .

In the same paper [1], the synthesis of the bifunctional catalyst $\text{Ni}^0/\text{La}_2\text{O}_3$ has been described in detail, showing the proximity between the 2 active sites of the 2 functions of the catalyst, i.e. " Ni^0 " and " $\text{La}-\text{O}$ ".

In our previous paper [2] the power rate laws of TOM, DRM and POM have been obtained and the corresponding orders to reactants, the apparent rate constants and the activation energies have been determined. In order to avoid problems of heat and mass transfers this study has been conducted using initial rates of reactions at very low conversions and low temperatures. The TOM catalytic cycle has been shown to be the slower one compared to the DRM one and it has been considered as the rate determining cycle (rdc) of the overall POM process.

In our latest paper [3] the catalytic pathway of methane combustion has been presented according to Haber et al. theory [4,5]. The sequences of elementary steps of dry and steam reforming of

* Corresponding author at: Saigon University, Faculty of Pedagogy of Natural Sciences, 273 An Duong Vuong Dis.5, HCMC, Vietnam.

** Corresponding author.

E-mail addresses: hutri.sgu@yahoo.com (T.H. Nguyen), agata.lamacz@pwr.edu.pl (A. Łamacz).

¹ Died on August 13th 2015.

² On leave from UPMC.

methane have been presented mainly based on Rostrup-Nielsen and Bak Hansen [6] and Wei and Iglesia [7,8] kinetic approach.

The present study is based on the theory of Classical Kinetics of heterogeneous catalytic reactions published in references [9] and [10a–b]. The basic concepts and definitions have been presented introducing the Quasi-Steady-State-Approximation (QSSA) [9–p.89,section 2]. How to obtain a good rate law in Kinetics of heterogeneous catalytic reactions has been described applying the Quasi-Steady State Approximation [9–p.90,section 2.3]. The concept of two-step catalytic reaction has then been described [9–p.91,section 2.4]. How to select the two steps has also been presented, on the basis of kinetically insignificant steps and far-equilibrium steps [9–p.91,section 2.5]. Moreover, the origin of the equality between the rates of catalytic steps in a catalytic cycle was described [9–p.92,section 2.6]. This equality is based on the concept of the “most abundant reaction intermediate” (“mari”) [9–p.91,section 2.3.3]. Furthermore, it is obvious that the “rate determining step” in a catalytic sequence is not a slow step, but a step which is generally producing or consuming the “mari” [9–p.92,section 2.5]. The definition of assisted catalytic processes has been developed [9–p.92,section 3]. It is the basis of our indirect model of POM process, which is based on 3 catalytic cycles turning over a bifunctional catalyst. The kinetic coupling in catalytic cycle has been introduced [9–p.95,section 4] and was applied in our POM model.

In this work we combined two aspects: (i) the experiments carried out at low conversion in order to avoid problems of mass and heat transfers and for calculating the rate of reactions (not the rate of diffusion); (ii) determination of initial rates permitting to calculate rate constants, order to reactants for power rate law (PRL) study, activation energy permitting to get the value of rate constant for POM reaction at high temperature. To determine initial rates of reactions, a classical differential micro-reactor was used for experiments. It basically means that in these conditions CH_4 and O_2 or CO_2 concentrations can be considered constant in kinetic equations. Consequently, the conversions of CH_4 , CO_2 or O_2 have to remain less than 5%. The conversions of 10% are too high for considering the concentration of reactant as constant in kinetic equations. It can also introduce deviation of the experimental data in relation to simulation plots, because concentrations or reactants cannot be considered as constant.

Several questions had then to be answered and they define the objectives of the present work:

- (i) In the case of power rate laws kinetics of TOM and DRM at low temperature and low methane conversion, the orders were found to vary with methane conversion and temperature, so the first aim is to extent the Quasi-Steady State-Approximation (QSSA) kinetics of TOM, DRM and POM at higher temperatures and conversions of methane to complete the kinetic study of the POM process occurring at 1053 K.
- (ii) Using the experimental data of our previous initial power rate laws, order to reactants, apparent rate constants and activation energies at low conversion and temperature, the objectives are:
 - To establish the classical rate equations at the molecular level (QSSA application) of TOM, DRM and POM permitting to extent the simulation of the 3 reactions to higher values of contact times, methane conversions and temperatures;
 - To compare the two power rate law equations and QSSA kinetic laws for TOM and DRM in order to interpret the significance of the apparent rate constants of the power rate laws;
 - To simulate kinetic plots of TOM, DRM and POM and check with the corresponding experimental data;
 - To show that the kinetic plot of POM depends on that of TOM.

2. Experimental

The bifunctional $\text{Ni}^0/\text{La}_2\text{O}_3$ catalyst was obtained from the transformation of LaNiO_3 perovskite in flowing mixture of POM ($\text{CH}_4/\text{O}_2 = 2$). The process of perovskite reduction to $\text{Ni}^0/\text{La}_2\text{O}_3$ was occurring via the reaction total oxidation of methane, in which oxygen from perovskite was used. The H_2 production was taking place only by the end of reduction of LaNiO_3 to $\text{Ni}^0/\text{La}_2\text{O}_3$. The LaNiO_3 reduction process has been described in great details in [1].

The catalytic device was a differential micro-reactor. In this work we combined two aspects: (i) working at low conversion in order to avoid problems of mass and heat transfers and obtaining rate of reactions (not rates of diffusion); (ii) to calculate initial rates permitting to determine rate constants, order to reactants (for PRL study), and activation energy permitting to get the value of rate constant for POM reaction at high temperature.

Kinetic experimental conditions of TOM, DRM, POM had been described in our previous paper [2]. As a summary, the catalytic rate studies of TOM, DRM and POM were performed by using catalyst samples (particle size of 250–425 μm) in a quartz tube reactor (6-mm inner diameter) equipped with an external type-K thermocouple at the level of the catalyst bed, with continuous gas flow at atmospheric pressure. Substrates, i.e. methane and oxygen or carbon dioxide, were diluted in helium, except for POM experiments argon was used. The experiments were carried out at different temperatures in isothermal conditions. Conversion degrees of methane less than 5–10% have been previously used [3] for determining the power rate law kinetic parameters. The concentration of reagents at the reactor outlet was determined using an on-line gas chromatograph equipped with a thermal conductivity detector (TCD).

The catalytic runs of TOM were carried out over 100 mg La_2O_3 catalyst density of 1 g/cm³) at three different temperatures: 773, 823 and 873 K, and for three different contact times (t_c): 0.06, 0.12 and 0.24 s, in order to remain at low conversion of methane.

The DRM reactions were studied over 100 mg $\text{Ni}^0/\text{La}_2\text{O}_3$ (density of 0.6 g/cm³), obtained by the in situ transformation of LaNiO_3 in flowing POM mixture [1]. The DRM reaction was carried out at four different temperatures: 648, 673, 698 and 723 K, and three different contact times: 0.1, 0.2 and 0.4 s.

For the kinetic studies of POM reaction, the stoichiometric CH_4/O_2 ratio of 2 (i.e. $[\text{CH}_4]/[\text{O}_2] = [0.4]/[0.2]$) in the flowing gas mixture was applied for all experiments. It was carried out over $\text{Ni}^0/\text{La}_2\text{O}_3$ at four different temperatures: 993, 1013, 1033 and 1053 K, using three different contact times: 0.0075, 0.01 and 0.015 s.

3. Results and discussion

3.1. Total oxidation of methane to $\text{CO}_2/\text{H}_2\text{O}$ over La_2O_3

The overall reaction is:



The power rate law is defined as

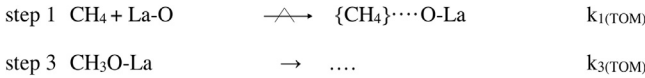
$$r_{\text{TOM}} = k_{\text{exp}(\text{TOM})}[\text{CH}_4]^\alpha[\text{O}_2]^\beta \quad (2)$$

The apparent rate constant $k_{\text{exp}(\text{TOM})}$ is defined in this work at the molecular level by identifying the power rate law to the detailed classical rate equation defined below. Let's remember that in our experimental conditions the β order to O_2 was found to be equal to zero [2]. It means that the active surface of La_2O_3 , where TOM is occurring, is saturated by oxygen species, which are the most abundant reactive intermediates of TOM.

3.1.1. The two-step sequence of TOM over La_2O_3

In the frame of the classical kinetic approach published by Boudart and Djéga-Mariadassou [9], the steps 1 and 3 of the com-

plete sequence of elementary steps published previously [3], and reported in Appendix, lead to the following two-step sequence:



where:

$\{\text{CH}_4\} \cdots \text{O-La}$ is the surface complex corresponding to the 1st step of methane chemisorption on La_2O_3 , and where $\text{CH}_3\text{O-La}$ is the adsorbed methoxy group resulting of the complete dissociative adsorption of methane owing to the proximity of an adjacent "La-O" surface active site;

$\xrightarrow{\text{---}}$ is the symbol of the rate determining step (rds) selected for developing the detailed rate equation [9].

Let's remember that the classical kinetics is based on the Quasi-Steady State Approximation (QSSA), which demonstrates the equality of the rates of all the elementary steps included in a catalytic cycle, taking into account their stoichiometric number σ [9]. Applying the QSSA theory, the rate of methane total oxidation is $r_{\text{TOM}} = r_{1(\text{TOM})}/\sigma_1 = r_{3(\text{TOM})}/\sigma_3$:

$$k_{1(\text{TOM})}[\text{CH}_4]^1[\text{La-O}]^1 = k_{3(\text{TOM})}[\text{CH}_3\text{O-La}] \quad (5)$$

According to the experimental zero order to dioxygen [3] the most abundant reactive intermediate ("mari") is "La-O".

Step 1 is consuming the *mari* and will be the rate determining step of TOM reaction according to [10]:

$$r_{\text{TOM}} = r_{1(\text{TOM})} = k_{1(\text{TOM})}[\text{CH}_4]^1[\text{La-O}]^1 \quad (6)$$

The concentration of active sites [La-O] has therefore to be calculated for obtaining the final classical rate equation, as was done below.

The balance on the total active sites [L] is:

$$[L] = [\text{La-}\square] + [\text{La-O}] + [\text{CH}_3\text{O-La}] + \dots \quad (7)$$

The power rate law zero order to O_2 [2] means that as soon as an oxygen vacancy [La- \square] is created it is rapidly saturated by a new oxygen species and consequently [La- \square] can be considered as very small. Other reactive adsorbed species can also be considered as minor intermediates at low concentrations.

Therefore [La-O] and [CH₃O-La] being the major surface adsorbed and reactive species, the balance of surface species is:

$$[L] \approx [\text{La-O}] + [\text{CH}_3\text{O-La}] \quad (8)$$

From Eqs. (5) and (7) the concentration of reactive oxygen species is:

$$[\text{La-O}] = \frac{[L] k_{3(\text{TOM})}}{k_{3(\text{TOM})} + k_{1(\text{TOM})}[\text{CH}_4]} \quad (9)$$

Using Eqs. (6) and (9) the classical rate equation of the total oxidation of methane over La_2O_3 is:

$$r_{\text{TOM}} = r_1 = \frac{[L] k_{3(\text{TOM})} \left(\frac{k_{1(\text{TOM})}}{k_{3(\text{TOM})}} [\text{CH}_4] \right)}{\left(1 + \frac{k_{1(\text{TOM})}}{k_{3(\text{TOM})}} [\text{CH}_4] \right)} \quad (10)$$

3.1.2. Significance of the apparent rate constant $k_{\text{exp}(\text{TOM})}$ of the power rate law Eq. (2): comparison with the classical kinetics rate equation (Eq. (10))

According to references [9,10], the ratio in Eq. (10):

$$\frac{\frac{k_{1(\text{TOM})}}{k_{3(\text{TOM})}} [\text{CH}_4]}{1 + \frac{k_{1(\text{TOM})}}{k_{3(\text{TOM})}} [\text{CH}_4]}$$

1 (3)

1 (4)

is the generalized Langmuir adsorption isotherm of methane which can be approximated by the means of:

$$\frac{k_{1(\text{TOM})}[\text{CH}_4]}{1 + \frac{k_{1(\text{TOM})}}{k_{3(\text{TOM})}}[\text{CH}_4]} = \text{const.} \times [\text{CH}_4]^n \quad \text{with } 0 < n < 1 \quad (11)$$

$$\text{with const} = k_{1(\text{TOM})}/k_{3(\text{TOM})} \quad (12)$$

Hence:

$$r_{\text{TOM}} = r_{1(\text{TOM})} = [L] k_{3(\text{TOM})} \text{const} \times [\text{CH}_4]^n = [L] k_{1(\text{TOM})} [\text{CH}_4]^n \quad (13)$$

Eq. (13) is equivalent to the power rate law of the overall equation $\text{CH}_4 + 2\text{O}_2 = \text{CO}_2 + 2\text{H}_2\text{O}$:

$$r_{\text{TOM}} = k_{\text{exp}(\text{TOM})} [\text{CH}_4]^\alpha [\text{O}_2]^\beta \text{ with } \beta = 0 \text{ and } 0 < \alpha < 1 \quad (2)$$

According to Eq. (13):

$$k_{\text{exp}(\text{TOM})} = [L] k_{1(\text{TOM})} \quad (14)$$

According to the Classical Kinetics [9,10] the rds is the step whose rate constant appears in the rate equation, i.e. $k_{1(\text{TOM})}$, which corresponds to the activation of methane with the formation of a surface complex between one surface oxygen and CH_4 [4,5]. The activation energy of TOM is corresponding to the first step, i.e. the activation of methane.

3.1.3. Simulations of methane total oxidation at 873 K

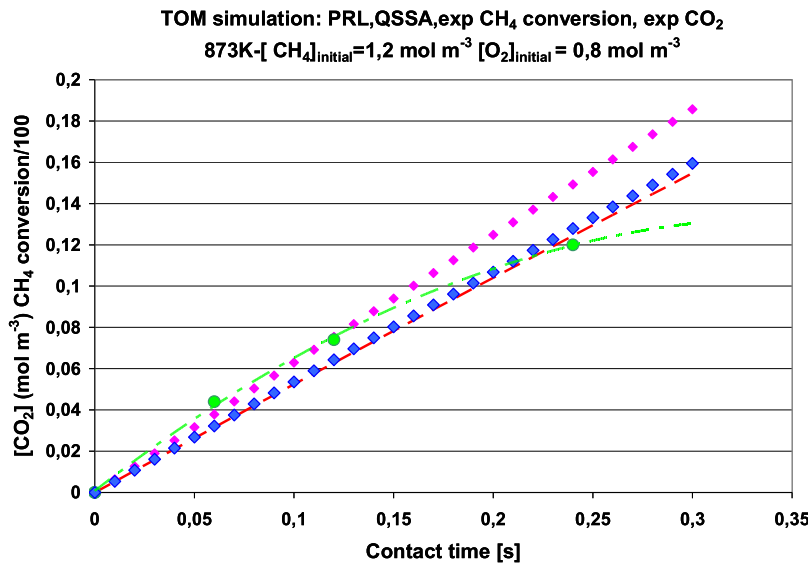
3.1.3.1. Power rate law simulation of methane total oxidation. The power rate law of TOM reaction has been studied in our previous paper [2]. For the reaction carried out in the following mixture $[\text{CH}_4] = 1.2$ and $[\text{O}_2] = 0.8$ (mol m^{-3}), the values of the apparent rate constant, reaction order to methane (α) and reaction order to oxygen (β), at 873 K were as follows: $k_{\text{TOM}(873)} = 0.6 \{(\text{mol m}^{-3})^{1-\alpha} \text{ s}^{-1}\}$, $\alpha = 0.35$, $\beta = 0$.

The power rate law simulation of TOM reaction based on the above data is presented in Fig. 1.

At the beginning of methane reaction, for contact time up to only 0.3 s, it can be observed that methane conversion is very low. The experimental conditions of TOM, low temperature leading to low conversion of reactants, were selected to avoid any problem of heat and mass transfer.

Using the power rate law equation, both calculated and experimental concentrations of CO_2 are presented on the simulated plot (Fig. 1). A very good fitting is observed for low contact times (i.e. 0.06 s and 0.12 s). The order to methane is practically constant in this low contact time domain. It is the useful domain of methane conversion for PRL calculation.

For higher methane conversion, i.e. at 0.24 s, a small deviation between the simulated plot and experimental value of CO_2 is appearing: it can be either due to too high value of conversion or to the evolution of the order to CH_4 for methane conversion higher than 10% as observed in [2]. Let's note that the statistical error between experimental and calculated values, or statistical error for the whole values of PRL and QSSA (Fig. 1), for the sake of comparison between the two equations with experimental data, is respectively between 0.03 and 0.01 mol m^{-3} . Each contact time corresponds to about 15 min time on run to observe steady state of the system. The initial rate (Fig. 1) is: $r^0_{\text{PRL}} = 0.62 \text{ mol m}^{-3} \text{ s}^{-1}$.



QSSA rate equation (15): $[L]k_{1(TOM)} = 0.6$; $k_{1(TOM)}/k_{3(TOM)} = 4.0$;
 PRL equation: $r_{TOM} = k_{exp\ TOM} [CH_4]^\alpha [O_2]^\beta$ with $\beta = 0$; $0 < \alpha < 1$;
 $k_{exp\ TOM} = [L] k_{1(TOM)}$.

Fig. 1. Power rate law (PRL) and Quasi-Steady State Approximation (QSSA) simulation of TOM at 873 K: (◆) [CO₂] PRL; (●) [CO₂] experimental; (◆) [CO₂] QSSA; (---) experimental CH₄ conversion; (—) tendency plots of experimental [CO₂].
 $[CO_2]_{QSSA} = 0.531 t_c$, $R^2 = 1$; $[CO_2]_{PRL} = 0.619 t_c$, $R^2 = 1$. $[CO_2]_{exp} = -1.061 t_c^2 + 0.750 t_c$, $R^2 = 0.99$. $r^0_{PRL} = 0.62 \text{ mol m}^{-3} \text{ s}^{-1}$; $r^0_{QSSA} = 0.53 \text{ mol m}^{-3} \text{ s}^{-1}$; $r^0_{QSSA\ high\ conversion} = 0.47 \text{ mol m}^{-3} \text{ s}^{-1}$ (see Fig. 2).

In order to avoid the evolution of the order to methane in simulation when using the power rate law, the application of the QSSA kinetic approach of the TOM process was developed. Using the link between the QSSA theory and the power rate law Eq. (11) and the resulting detailed equation Eq. (10) an equivalent simulation can be reported (Fig. 1).

3.1.3.2. Classical kinetics (QSSA) simulation of methane total oxidation. The classical kinetic equation is based on Eq. (10):

$$r_{TOM} = r_{1(TOM)} = \frac{[L]k_{3(TOM)} \left(\frac{k_{1(TOM)}}{k_{3(TOM)}} [CH_4] \right)}{(1 + \frac{k_{1(TOM)}}{k_{3(TOM)}} [CH_4])} = [L]k_{1(TOM)} \frac{[CH_4]}{1 + \frac{k_{1(TOM)}}{k_{3(TOM)}} [CH_4]} \quad (15)$$

with, $[L]k_{1(TOM)} = k_{exp(TOM)} = 0.6 \text{ (mol m}^{-3}\text{)}^{1-\alpha} \text{ s}^{-1}$ [2]; and, according to simulation, $k_{1(TOM)}/k_{3(TOM)} = 0.25$.

The simulated plots of TOM reaction corresponding to classical (QSSA) kinetic equation (Eq. (15)) at 873 K are presented in Fig. 2 for higher contact times (up to 4.5 s) and in Fig. 3 for lower contact times (0.4 s). Let's note that the classical kinetic equation describes the reaction without considering heat and mass transfers up to higher conversions.

As it can be seen in Fig. 1, simulated and experimental data are quite consistent and the simulated initial rate of TOM is equal to the experimental initial one, i.e. 0.53 (mol m⁻³ s⁻¹).

Owing to the classical kinetic equation (Eq. (15)), Fig. 2 shows the methane conversion almost up to 100%. The concentrations of CH₄ and CO₂ versus contact time up to 4.5 s are plotted. It can be observed that the complete methane conversion can be expected for $t_c > 3$ s. Furthermore, the initial rate is 0.47 mol m⁻³ s⁻¹, which is quite near to the rate presented in Fig. 1.

3.2. Dry reforming of methane over Ni⁰/La₂O₃

In our indirect POM model [1–23] dry and steam reforming are two kinetically coupled reactions, turning over with the same rate, as discussed in literature and in our previous paper [2]. The rds of both cycles is the same: the methane dehydrogenation. Consequently, dry reforming alone has been simulated in the present work and it will permit to simulate the POM process in section 5 of this paper, taking into account the equality of DRM and SRM rates of reaction.

The overall reaction is:



The power rate law is defined as:

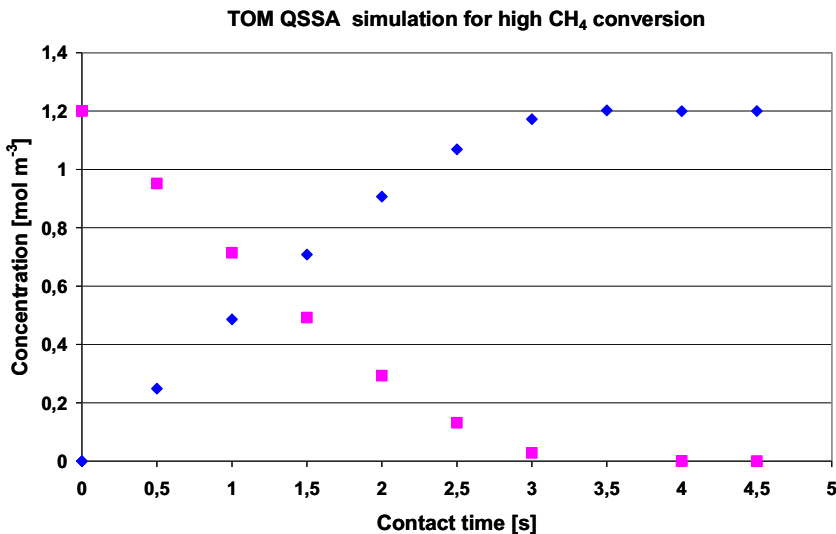
$$r_{DRM} = k_{exp(DRM)} [CH_4]^\gamma [CO_2]^\delta \quad (17)$$

As for the total oxidation of methane, the apparent rate constant $k_{exp(DRM)}$ will be defined at the molecular level, by identifying the power rate law Eq. (17) to the detailed classical rate equation (QSSA). It is worth noting that the sum $(\delta + \gamma)$ has been found to be experimentally equal to 1. It will be demonstrated in the next section.

3.2.1. The two-step sequence of elementary steps for DRM

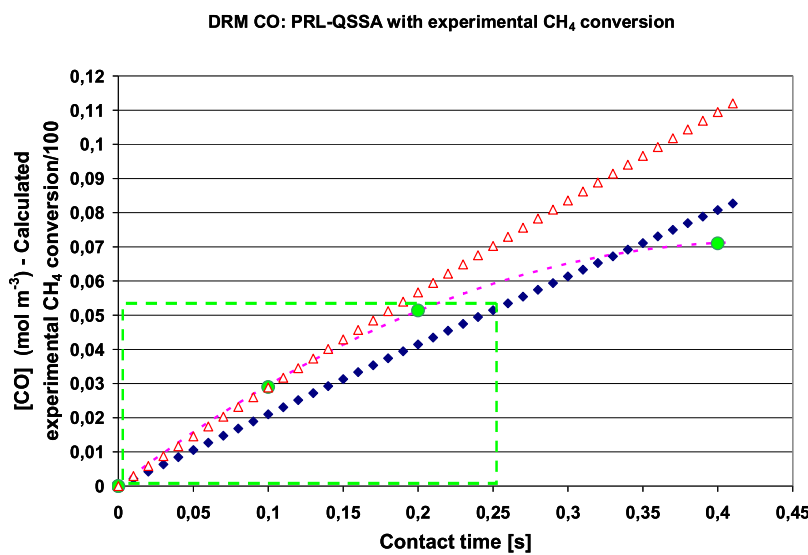
The complete sequence of elementary steps defining the catalytic cycle of the dry reforming of CH₄ was defined in our previous paper [3] and is reported in the Appendix.

Taking into account the results of the power rate law on methane and dioxygen kinetic behaviors, the following 2 elementary steps can be selected for determining the classical kinetic rate law of DRM at the molecular level, applying the QSSA theory.



$$\text{QSSA rate equation (15): } [L]k_{1(\text{TOM})} = 0.6 ; k_{1(\text{TOM})}/k_{3(\text{TOM})} = 4$$

Fig. 2. Classical kinetics-QSSA simulation of TOM for higher contact time, at 873 K, for determining total flow rate mixture and catalyst volume to obtain high reactant conversion. (◆) [CO₂], (■) [CH₄]. [CH₄]_{initial} = 1.2 mol m⁻³. [O₂]_{initial} = 0.8 mol m⁻³. Tendency plot of [CO₂]_{initial} = 0.472 t_c + 0.006; R² = 0.99. Initial rate: r⁰ = 0.47 mol m⁻³ s⁻¹.



$$\text{QSSA rate equation(30): } [L]k_{1(\text{DRM})} = 0.36 ; k_{1(\text{DRM})}/k_{3(\text{DRM})} = 0.35 ; \text{PRL equation (17): } k_{\text{DRM}} = 0.36; \gamma = 0.64; \delta = 0.34; 698\text{K}$$

Fig. 3. Simulation of CO QSSA and PRL at low CH₄/CO₂ conversion in DRM at 698 K. (●) [CO] experimental; (△) CO PRL; (◆) CO QSSA; (—) CH₄ conversion = -0.391 t_c² + 0.334 t_c = R² = 1 (experimental CO equation tendency); [] is the domain of validity for differential micro-reactor calculation (PRL) with methane conversion \leq 5–6%.

[CH₄]_{initial} = [CO₂]_{initial} = 0.4 mol m⁻³. [CO]_{PRL} = 0.2736 t_c; R² = 0.999. r⁰_{PRL} = 0.27 mol m⁻³ s⁻¹. [CO]_{QSSA} = 0.202 t_c; R² = 0.999. r⁰_{QSSA} = 0.20 mol m⁻³ s⁻¹.



3.2.2. Classical kinetic rate law of DRM at the molecular level

According to the kinetic methodology in 3 stages [9], it comes:

- (i) applying the QSSA: $r_{1(\text{DRM})} = r_{3(\text{DRM})}$;
- (ii) the two steps being far equilibrium, equilibrium constants cannot be used for the kinetics;
- (iii) the balance on the density of sites [L] can be done on the main adsorbed species of the two steps:

$$[L] = [*] + [*\text{CH}_4] + [*\text{CO}] + \text{non kinetically significant adsorbed species} \quad (20)$$

Coming back to the rate equations:

$$(21) \quad r_{\text{DRM}} = r_{1(\text{DRM})} = k_{1(\text{DRM})}[\text{CH}_4]^1[*]^1 = r_{3(\text{DRM})} = k_{3(\text{DRM})}[\text{CO}_2]^1[*]^1$$

According to the two-steps general equation of Temkin and Boudart [10]:

$$r_{\text{DRM}} = \frac{[L]k_{1(\text{DRM})}[\text{CH}_4]k_{3(\text{DRM})}[\text{CO}_2] - k_{-1(\text{DRM})}[*\text{CH}_4]k_{-3(\text{DRM})}[*\text{CO}_2]}{k_{1(\text{DRM})}[\text{CH}_4] + k_{-1(\text{DRM})}[*\text{CH}_4] + k_{2(\text{DRM})}[\text{CO}_2] + k_{-3(\text{DRM})}[*\text{CO}_2]} \quad (22)$$

As steps [1] and [3] are far equilibrium, r_{DRM} equation (Eq. (22)) becomes:

$$r_{\text{DRM}} = \frac{[L]k_{1(\text{DRM})}[\text{CH}_4]k_{3(\text{DRM})}[\text{CO}_2]}{k_{1(\text{DRM})}[\text{CH}_4] + k_{3(\text{DRM})}[\text{CO}_2]} \quad (23)$$

Using step [1] (Eq. 18) for calculation (let's note that similarly step 2 can be used and will lead to the same result):

$$r_{\text{DRM}} = [L]k_{3(\text{DRM})}[\text{CO}_2] \frac{\frac{k_{1(\text{DRM})}[\text{CH}_4]}{k_{3(\text{DRM})}[\text{CO}_2]}}{\left(1 + \frac{k_{1(\text{DRM})}[\text{CH}_4]}{k_{3(\text{DRM})}[\text{CO}_2]}\right)} \quad (24)$$

3.2.3. Significance of the apparent rate constant $k_{\text{exp}(\text{DRM})}$ of the power rate law equation by comparison with the classical equation

In Eq. (24) the ratio:

$$\frac{\frac{k_{1(\text{DRM})}[\text{CH}_4]}{k_{3(\text{DRM})}[\text{CO}_2]}}{1 + \frac{k_{1(\text{DRM})}[\text{CH}_4]}{k_{3(\text{DRM})}[\text{CO}_2]}}$$

is the generalized Langmuir adsorption isotherm [9], which can be approximated by the means of:

$$\frac{\frac{k_{1(\text{DRM})}[\text{CH}_4]}{k_{3(\text{DRM})}[\text{CO}_2]}}{1 + \frac{k_{1(\text{DRM})}[\text{CH}_4]}{k_{3(\text{DRM})}[\text{CO}_2]}} = \text{const.} \left(\frac{[\text{CH}_4]}{[\text{CO}_2]} \right)^n \quad \text{with} \quad 0 < n < 1 \quad (25)$$

and

$$r_{\text{DRM}} = [L]k_{3(\text{DRM})}[\text{CO}_2] \text{const.} \left(\frac{[\text{CH}_4]}{[\text{CO}_2]} \right)^n \quad (0 < n < 1) \quad (26)$$

Where, $\text{const.} = k_{1(\text{DRM})}/k_{3(\text{DRM})}$ (27)

$$r_{\text{DRM}} = [L]k_{1(\text{DRM})}[\text{CH}_4]^n[\text{CO}_2]^{(1-n)} \quad (28)$$

Then, $r_{\text{DRM}} = k_{\text{DRM}}[\text{CH}_4]^\gamma[\text{CO}_2]^\delta$ (17)

$$\Rightarrow k_{\text{DRM}} = [L]k_{1(\text{DRM})} \quad (29)$$

with $n = \gamma$, and $(1 - n) = \delta$, the global order $(\gamma + \delta)$ of DRM reaction should be always equal to 1, which observed experimentally.

3.2.4. Simulations of the methane dry reforming reaction at 698 K

3.2.4.1. Power rate law (PRL) simulation of methane dry reforming. The overall DRM equation is described by Eq. (16). The power rate law equation is presented by Eq. (17). It is worth noting that the sum $(\gamma + \delta)$ has been found to be experimentally equal to 1 as claimed above and also expected in classical kinetics in the next section.



$$r_{\text{DRM}} = k_{\text{exp}(\text{DRM})}[\text{CH}_4]^\gamma[\text{CO}_2]^\delta \quad (17)$$

In our previous paper [2], for DRM reaction at 698 K with the following reagent concentrations: $[\text{CH}_4] = 0.4$; $[\text{CO}_2] = 0.4$ (mol m^{-3}), it has been calculated that the values of the rate constant: $k_{\text{DRM}(698)} = 0.3$ ($\text{mol m}^{-3} \text{s}^{-1}$), the reaction order to methane: $\gamma = 0.65$ and reaction order to CO_2 : $\delta = 0.34$. The power rate law simulation of DMR reaction (Fig. 3) was calculated at 698 K using the above data.

Both calculated and experimental concentrations of CO are reported on the simulated plot (Fig. 3) using the power rate law equation. A very good fitting is observed at low contact times (i.e. 0.1 and 0.2 s) as they are in the domain of validity of the initial rate protocol in the differential micro-reactor. The orders to methane and CO_2 are practically constant in these cases. For higher contact time (i.e. 0.4 s), a deviation between simulated plot and experimental value of CO is appearing. For methane or carbon dioxide conversion higher than 5%, the order to methane and carbon dioxide can be different. Let's note that the absence of any drastic catalyst deactivation is expected as already discussed in [3]. The initial rate is: $r^0_{\text{PRL}} = 0.27 \text{ mol m}^{-3} \text{s}^{-1}$. As for TOM simulation, both the variation of orders to methane and carbon dioxide and too high conversion justify the application of the classical kinetic approach for simulating the reaction at higher conversions, as presented in next section.

3.2.4.2. Classical kinetic (QSSA) simulation of methane dry reforming. The classical kinetic simulation of DRM reaction (with $[\text{CH}_4] = 0.4$; $[\text{CO}_2] = 0.4 \text{ mol m}^{-3}$) is based on Eq. (24) at 698 K:

$$r_{\text{DRM}} = [L]k_{3(\text{DRM})}[\text{CO}_2] \frac{\frac{k_{1(\text{DRM})}[\text{CH}_4]}{k_{3(\text{DRM})}[\text{CO}_2]}}{\left(1 + \frac{k_{1(\text{DRM})}[\text{CH}_4]}{k_{3(\text{DRM})}[\text{CO}_2]}\right)} = [L]k_{1(\text{DRM})} \frac{[\text{CH}_4]}{\left(1 + \frac{k_{1(\text{DRM})}[\text{CH}_4]}{k_{3(\text{DRM})}[\text{CO}_2]}\right)} \quad (30)$$

where,

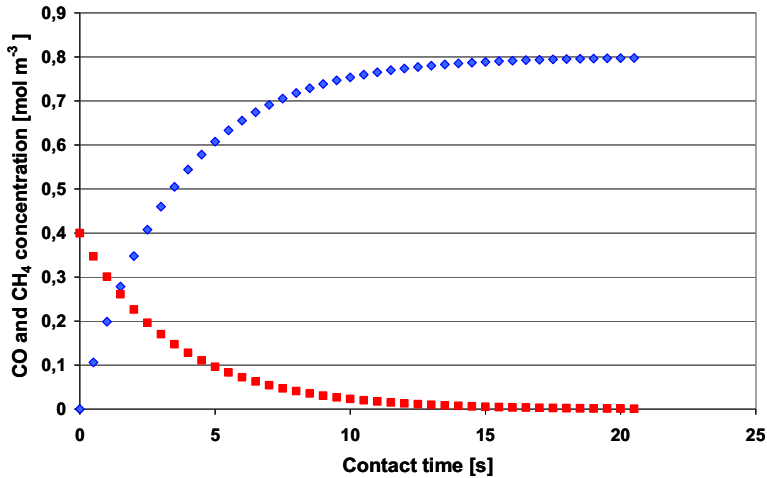
$[L]k_{1(\text{DRM})} = k_{\text{exp}(\text{DRM})} = 0.3$ [2] and according to simulation: $k_{1(\text{DRM})}/k_{3(\text{DRM})} = 0.355$.

The simulated plots of DRM reaction corresponding to the classical kinetic equation (Eq. (30)) are presented in Fig. 4. In the classical kinetic equation, the effects of heat, mass transfer and order to methane are absent as it has been done in the case of TOM.

The simulated plot of classical kinetic equation in Fig. 3 corresponds to very low methane and carbon dioxide conversion at contact times up to 0.4 s only. It is observed that both simulated and experimental concentrations of CO are consistent. The initial rate is $r^0_{\text{PRL}} = 0.20 \text{ mol m}^{-3} \text{s}^{-1}$.

Higher conversions of methane and carbon dioxide are shown in Fig. 4, where concentrations of CH_4 , CO_2 and CO were calculated for contact times up to 20 s. It can be observed that the complete methane or carbon dioxide conversion should occur for $t_c > 20$ s. The initial rate $r^0 = 0.19 \text{ mol m}^{-3} \text{s}^{-1}$, as was found for low methane conversion.

QSSA Simulation of DRM for high conversion



$$\text{QSSA rate equation (30): } [L] k_{1(\text{DRM})} = 0.36 ; k_{1(\text{DRM})}/k_{3(\text{DRM})} = 0.35 ;$$

Fig. 4. Simulation of the classical kinetics-QSSA of DRM for higher contact time, at 698 K, for determining total flow rate mixture and catalyst volume to obtain high CH₄/CO₂ conversion. Contact time (s) = Volume of catalyst (m³)/Total Flow rate (m³/s).

[CH₄]_{initial} = [CO₂]_{initial} = 0.4 mol m⁻³. (■) CH₄ (or CO₂); (◆) CO. Initial rate r⁰ = 0.19 mol m⁻³ s⁻¹ ([CO]_{init} = 0.198 tc; R² = 0.99).

3.3. Simulation of POM process at 1053 K. Comparison with the simulation of TOM assumed to be the rate determining cycle (rdc) of POM [2]

The values of the initial rates of POM have been already obtained at different temperatures, and Arrhenius laws for both TOM and POM reactions have been determined [2]:

$$\text{For TOM: } \ln k_{\text{TOM}} = 15.56 - \frac{116,422}{8,32*T} \quad (36)$$

$$\text{For POM: } \ln k_{\text{POM}} = 16.02 - \frac{112,811}{8,32*T} \quad (37)$$

Using Arrhenius laws for both TOM Eq. (36) and POM Eq. (37) reactions at 1053 K:

$$k_{\text{TOM}} = 9.68 \{(\text{mol m}^{-3})^{1-\alpha} \text{ s}^{-1}\}$$

$$k_{\text{POM}} = 23.18 \{(\text{mol m}^{-3})^{1-\alpha} \text{ s}^{-1}\}$$

The initial rate of POM at 1053 K is:

$$d[\text{CO}]/dt = 22.5 \{(\text{mol m}^{-3})^{1-\alpha} \text{ s}^{-1}\}.$$

and it has also been previously shown [2] that k_{POM} ≈ 2 k_{TOM}.

- (i) the factor 2 between k_{POM} and k_{TOM}, due to the kinetic coupling of the steam and dry reforming cycles turning over at the same rate in agreement with literature [7,8];
- (ii) and the stoichiometric relation between CO₂ produced by TOM and CO produced by both the dry reforming reaction (using CO₂ from TOM) and steam reforming reaction (consuming H₂O from TOM).

The classical equation used for simulating TOM reaction and calculating [CH₄] and [CO₂] is:

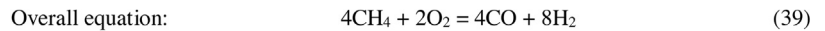
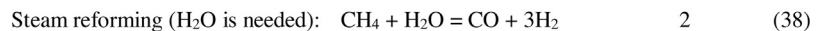
$$r_{\text{TOM}} = r_{1(\text{TOM})} = \frac{[L] k_{3(\text{TOM})} \left(\frac{k_{1(\text{TOM})}}{k_{3(\text{TOM})}} [\text{CH}_4] \right)}{\left(1 + \frac{k_{1(\text{TOM})}}{k_{3(\text{TOM})}} [\text{CH}_4] \right)} = \frac{d[\text{CO}_2]}{dt} \quad (12)$$

with,

$$[L] k_{3(\text{TOM})} = 12 \{(\text{mol m}^{-3})^{1-\alpha} \text{ s}^{-1}\}, \text{ and } [\text{CH}_4]_{\text{initial}} = 0.4 \{(\text{mol m}^{-3})\}.$$

We know that [L] k_{1(TOM)} = k_{exp(TOM)} = 9.68, and the simulation leads to k_{1(TOM)}/k_{3(TOM)} = 0.8. Hence, we can get the value of [L] k_{3(TOM)} = 12 {(\text{mol m}^{-3})^{1-\alpha} \text{ s}^{-1}}.

The simulated concentration of [CO] for POM reaction is 4 times that from [CO₂] according to the sequence of reactions in the POM model [1,3]:



It can be seen that for 1 CO₂ produced in TOM (Eq. (1)), 4 CO are resulting after the dry (2 CO, Eq. (18)) and steam (2 CO, Eq. (38)) with σ = 2) reactions.

In Fig. 5 the plot of CH₄ and CO₂ resulting from the TOM reaction (Eq. (1)) were first calculated.

If TOM is the rdc it should give the rate of POM reaction. The simulations of CO₂ (from TOM) and CO production from POM have therefore to be compared taking into account:

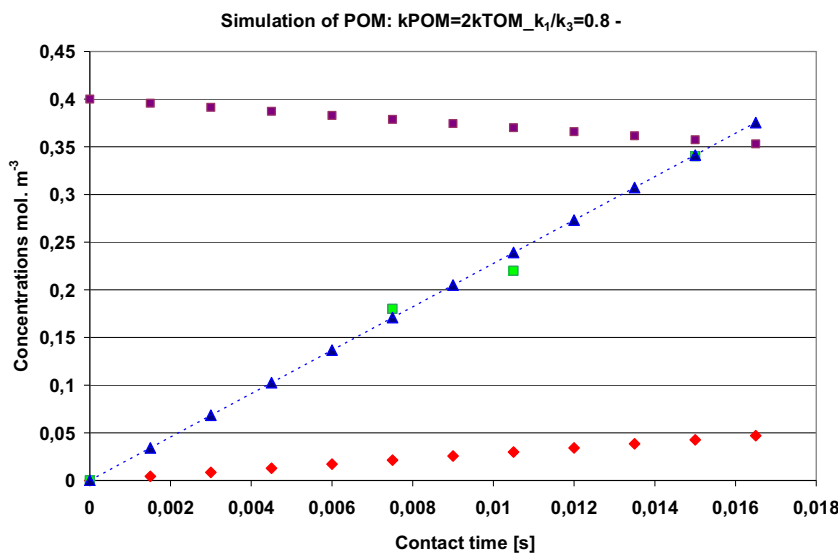


Fig. 5. Comparison between $[CO_2]$ of TOM using QSSA equation and $[CO]$ of POM experiment at 1053 K. (◆) $[CO_2]$; (▲) $[CO] = 2 \times 4 [CO_2]$; (■) Experimental $[CO]$ in POM; (■) $[CH_4]$; $[CH_4]_{initial} = 0.4 \text{ mol m}^{-3}$; order to $O_2 = 0$.

Considering: $r_{POM} = d[CO]/dt$ and $r_{TOM} = d[CO_2]/dt$ as measured in Fig. 5,

- (i) Stoichiometrically, $r_{POM} = d[CO]/dt = d\{4[CO_2]\}/dt$
- (ii) Kinetically, due to the DRM and SRM kinetic coupling, the overall POM rate is multiplied by a factor ≈ 2 , the rates of SRM and DRM being recognized to be equal, the rate determining steps being those of CH_4 dehydrogenation (2, 6–8) (see Annex). The fundamental equation is therefore:

$$r_{POM} = d[CO]/dt = 2 * d\{4 * [CO_2]\}/dt = 8 * d[CO_2]/dt.$$

It means that $r_{POM}^0 = 8 * r_{TOM}^0$.

This is confirmed by the two tendency equations of $[CO]$ and $[CO_2]$ vs t_c in Fig. 5:

$$\begin{aligned} [CO] &= 22,747 * t_c \quad (R^2 = 1) \quad r_{initPOM}^0 = 22.75 \text{ mol m}^{-3} s^{-1} \\ [CO_2] &= 2,8434 * t_c \quad (R^2 = 1) \quad r_{initTOM}^0 = 2.84 \text{ mol m}^{-3} s^{-1} \end{aligned}$$

with $2.84 * 8 = 22.72$.

Finally, the data from the experimental value of CO at 1053 K were reported [2].

As it can be seen, there is a perfect agreement between the POM and simulated values of CO at 1053 K. Furthermore, the initial rate of simulated plot of CO_2 vs. t_c is equal to the initial rate of experimental POM [2]: $22.5 \text{ (mol m}^{-3} \text{ s}^{-1}\text{)}$ for both of them, as presented above.

4. Conclusion

The POM model involved two basic catalytic cycles, with CO_2 as a product of TO and CO as a product of DRM reaction. The simulated graphs of TOM and DRM reactions were studied. The rate of TOM was used for calculating the rate of POM and the role of DRM, similar to that of SRM, was used to determine two parameters of the POM rate equation, based on the stoichiometry of POM and the kinetic coupling of DRM and SRM assisted by TOM.

Classical kinetics [9], based on the application of the QSSA theory and the concept of two-step sequence of elementary steps has permitted to establish the rate equation at the molecular level of TOM and DRM reactions. It allows to extent the simulation of TOM, DRM and POM reactions to higher contact times, methane conver-

sion and temperatures. The kinetic link between the power rate laws and detailed kinetic laws of TOM and DRM reactions was established. The experimental values of CO_2 from TOM reaction at 873 K, CO from DRM reaction at 698 K and the simulated graphs of TOM/DRM reactions were shown to be quite consistent too. The perfect agreement between the experimental values of CO from POM, and CO from simulated POM reaction at 1053 K was demonstrated. Furthermore, the initial rate of the simulated plot of CO_2 vs t_c is equal to the initial rate of POM experimental value, i.e. $22.5 \text{ (mol m}^{-3} \text{ s}^{-1}\text{)}$. It has been proven again that the rate of TOM catalytic cycle is the *rate determining cycle (rdc)* of the overall POM process, taking into account the stoichiometry of reactions in the POM model.

The bifunctional Ni/La_2O_3 catalyst has three main characteristics: (i) one of the best transition metal for methane dehydrogenation, (ii) a quite active catalyst for methane oxidation (La_2O_3), and (iii) the synthesis of this bifunctional catalyst leads to a very good proximity of the two functions of POM reaction, i.e. methane oxidation and methane reforming [1]. Optimisation of POM catalyst in the future can be based on the present model, considering that reaction of methane combustion provides the rate determining catalytic cycle (rdc) of the POM process.

Acknowledgements

Dr. M. Lewandowski is greatly acknowledged for providing lanthanum oxide material.

The Institute of General and Ecological Chemistry of Lodz University of Technology is gratefully acknowledged for support to Tri Huu Nguyen to develop global kinetics (power rate laws) of TOM and DRM.

The government of Vietnam is gratefully acknowledged for the grant (4915/QD-BGDDT) given to Tri Huu Nguyen to realize this work in Poland.

The work was partly financed by a statutory activity subsidy from the Polish Ministry of Science and Higher Education for the Faculty of Chemistry of Wrocław University of Technology.

This paper is dedicated to our co-author Dr. Andrzej Krzton, who died on August 13th 2015.

Appendix A.

Sequence of elementary steps of total oxidation of CH_4 [3]

[1]	$\text{CH}_4 + \text{La-O} \rightarrow \{\text{CH}_4\} \cdots \text{O-La}$	k_1	1
[2]	$\{\text{CH}_4\} \cdots \text{O-La} + \text{La-O} \rightarrow \text{CH}_3\text{O-La} + \text{La-OH}$	k_2	1
[3]	$\text{CH}_3\text{O-La} \rightarrow \dots$	k_3	1
(other unspecified, kinetically no significant steps leading to the reaction products CO_2 and H_2O)			
[10-p 98]			
[4]	$2 \text{La-O} + \text{O}_2 \rightarrow 2 \text{La-O}$	k_4	2

Overall equation: $\text{CH}_4 + 2\text{O}_2 = \text{CO}_2 + 2\text{H}_2\text{O}$

Sequence of elementary steps of methane dry reforming reaction [3]

Methane activation (“dehydrogenation”):

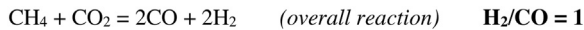
$\text{CH}_4(\text{gas}) + 2* \rightarrow \text{CH}_3* + \text{H}^*$	σ
	1
$\text{CH}_3* + * \rightarrow \text{CH}_2* + \text{H}^*$	1
$\text{CH}_2* + * \rightarrow \text{CH}^* + \text{H}^*$	1
$\text{CH}^* + * \rightarrow \text{C}^* + \text{H}^*$	1

CO_2 activation:

$\text{CO}_2 + * \rightarrow \text{CO}_2^*$	1
$\text{CO}_2^* + * \rightarrow \text{CO}^* + \text{O}^*$	1
$\text{CO}^* \rightarrow \text{CO} + *$	1

Surface reactions:

$\text{C}^* + \text{O}^* \rightarrow \text{CO}^* + *$	1
$\text{CO}^* \rightarrow \text{CO} + *$	1
$\text{H}^* + \text{H}^* \rightarrow \text{H}_2 + 2^*$	2



References

- [1] T.H. Nguyen, A. Łamacz, P. Beaunier, S. Czajkowska, M. Domański, A. Krztoń, T.V. Lê, G. Djéga-Mariadassou, Appl. Catal. B 152 (2014) 360.
- [2] T.H. Nguyen, A. Łamacz, A. Krztoń, A. Ura, K. Chałupka, M. Nowosielska, J. Rynkowski, G. Djéga-Mariadassou, Appl. Catal. B 165 (2015) 389.
- [3] T.H. Nguyen, A. Łamacz, A. Krztoń, B. Liszka, G. Djéga-Mariadassou, Appl. Catal. B 182 (2016) 385.
- [4] J. Haber, M. Witko, J. Catal. 216 (2003) 416.
- [5] J. Haber, W. Turek, J. Catal. 190 (2000) 320.
- [6] J.R. Rostrup-Nielsen, J.-H. Bak Hansen, J. Catal. 144 (1993) 38.
- [7] J. Wei, E. Iglesia, J. Catal. 224 (2004) 370.
- [8] J. Wei, E. Iglesia, J. Catal. 225 (2004) 116.
- [9] G. Djéga-Mariadassou, M. Boudart, J. Catal. 216 (2003) 89.
- [10] (a) M. Boudart, G. Djéga-Mariadassou, Cinétique des Réactions en Catalyse Hétérogène, Masson et Cie, Paris, 1982.